Natural Resources for Human Health

visaga publishing house

Original Research

View Article Online

Check for updates

Received 07 July 2023
Revised 22 July 2023
Accepted 25 July 2023
Available online 23 August 2023

Edited by Rohit Sharma

KEYWORDS:
Rust iron
IONPs
Environmental friendly
Aloe vera
MB dye

Natr Resour Human Health 2023; 3 (3): 355-363
https://doi.org/10.53365/nrfhh/170025
eISSN: 2583-1194
Copyright © 2023 Visagaa Publishing House

Study the degradation and photocatalytic activity of the methylene blue dye by mixing the Aloe vera extract with rust iron oxide nanoparticle

Duha A. Kadhim [1,*], Muslim A. Abid [1], Wafaa Mahdi Salih [1]

[1]Department of Physics, College of Science, Mustansiriyah University, Baghdad, Iraq

ABSTRACT: Iron oxide nanoparticles (IONPs) have been widely used in environmental applications due to their low cost, safety, and effectiveness. This research successfully produced IONPs by hydrothermally reacting iron rust and Aloe vera gel plant extract at 100 ^{o}C for 18 hours in an autoclave cell. IONPs were produced to prevent detrimental effects on human health by degrading methylene blue dye (MB). IONPs were characterized by XRD, FE-SEM, and FT-IR spectroscopy. The small crystalline size (19 nm), and (inverse cubic) structure (magnetite) of (Fe_3O_4 NPs) 600 ^{o}C were explained by measurements of XRD, whereas small crystalline ($Fe_{902}O$) NPs of 300 ^{o}C were of 28 nm. FESEM revealed that the particle size of (Fe_3O_4) NPs at 600 ^{o}C using an aloe vera extract was (26.80 to 37.96) nm, whereas $Fe_{902}O$ (wustite) at 300 ^{o}C was tiny and crystalline at (31.63 to 130.3) nm. The strong absorption band for Fe_3O_4 NPs (magnetites) at 600 °C with aloe vera is explained by the FT-IR spectra. The absorption peak was high at (650) cm-1 and corresponded to the Fe-O series of $Fe_{902}O$ NPs at 300 ^{o}C. When the spectra showed the absorption peak, it was strong. Iron oxide NPs have been used for a short time in environmental treatment to remove MB dye. For 40 minutes of IONPs (Fe_3O_4), the results of degradation effectiveness (95%) were 300 ^{o}C for MB dye, but degradation efficiency (91%) was 75 minutes of IONPs ($Fe_{902}O$) with aloe vera at 600 ^{o}C for MB dye.

1. INTRODUCTION

The term ”nanoparticles” (NPs) refers to small, inorganic or organic particles having a diameter of less than 100 nm that have unique features when compared to bulk materials (Xue et al., 2021). In comparison to other materials, (Herlekar et al., 2014) iron oxide (IONPs) comprise required materials with significant future advantages (Herlekar et al., 2014), different physical qualities such as low toxicity, powerful catalytic activity, small size, and a variety of physical properties (Cornell & Schwertmann, 2006; Guo et al., 2012; Issa et al., 2013). Human activity is now connected with chemicals in many aspects of life, and these compounds are damaging to the human body. Notably, some such compounds are continuously utilized, which is acknowledged as not being a ”completely safe chemical and not in return.” There is a substance that is extremely hazardous. Chemists in the Middle Ages were affected by the damage to explosive and toxic substances, and severe environmental problems began in the 17^{th} century as a result of mining cinder released in Germany, and pigment and other chemicals from carbon tar were released in the 18th century, leading to mine discharge. The overwhelming usage of iron metal led to the foundation of a waste yard of a thousand tons of rusty scrap and rubbish without any resolution to reuse it or take advantage of it until today, causing a dangerous environmental issue in various places in the world. In the summer, the iron consumed and the enormous quantities thereof constituted an environmental burden and have become a significant disposal difficulty. The MB dyes are among the many organic pollutants of water sources, and the reason for this is because they are of great importance and have wide use in various industries, as they are used in the textile industries, in printing, in photographic colors, as additives in the petroleum industries, etc. (Aliasghari et al., 2021; Maleki et al., 2015; Ren et al., 2021; Rominiyi et al., 2020; Taghipour, 2004). As a result, the presence of MB dye in wastewater is both undesirable and illegal, thus it is advisable to remove these components from the water before reintroducing them into the environment. This might be related to the aesthetics of the surroundings, the toxicity of pigments, and the long-term consequences on the environment and human body (Bedin et al., 2016; Djilani et al., 2015; Zhao et al., 2018). Economic efficiencies, nuclear economy, simplicity, benignity, non-toxicity, elimination of poisonous and harmful chemicals, ease of availability, and removal of ecologically hazardous elements make the green synthesis of the IONPs employed in biological components by plant extracts a major issue (Chamorro et al., 2020; Fallah et al., 2019; Yew et

* Corresponding author.
E-mail address: duha.abdual@uomustansiriyah.edu.iq (Duha A. Kadhim)

This is an open access article under the CC BY-NC-ND license (http://creativecommons.org/licenses/by-nc-nd/4.0/).

al., 2018). For millennia, people have recognized and used the aloe vera plant for its health, beauty, and skin benefits. The name Aloe vera is derived from the Arabic word "Alloeh," which means "shining bitter substance," and the Latin word vera," meaning "true." 2000 years ago, Greek scientists believed that aloe vera was a universal cure-all. The Egyptians referred to aloe as "the plant of immortality." Aloe vera is being used in a range of environmental therapies. Aloe vera Burm F., also known scientifically as Aloe barbadensis Miller, is a xerophytic plant with succulent leaves. The leaves are divided into three layers: a fleshy inner layer, a thin middle layer, and a thick protective outer layer. The outside layer is composed mostly of cellulose, the middle layer is dominated by barbaloin (aloin A and B), and the inner gel is composed primarily of acemannan, an acetylated glucomannan (Rahmani et al., 2020). The inner gel also contains carbohydrates, anthraquinones, amino acids, vitamins, and proteins (Kato, 2011; Roy & Das, 2015). Several previous studies have employed aloe vera gel to generate antibacterial edible films (Sharma et al., 2022), aloe-cellulose composite membranes (El-Baky et al., 2016), and antibacterial nonwoven textiles (Ghayempour et al., 2016). Additionally, the function of acemannon in the creation of nanoscaffolds with antibacterial activity is described. Among the most important types of metal oxide nanoparticles are ferric oxide nanoparticles (FONPs), which have magnetic characteristics, biocompatibility, and a high surface-to-volume ratio (Khatami, 2019). As a result, they are used in a range of environmental applications, including catalysis and the removal of heavy metals, antibiotics, and other colors from wastewater (Samira & Carvalho, 2017).

This work is examined in the literature: In T and Reihaneh (2021) study, an environmentally friendly technology was successfully used to create superparamagnetic (SPIONs), which were shown to have modest ranges of sizes. The production and characterization of IONPs from iron salts in the aqueous extracts of flaxseed and aloe vera leaves, which were accomplished using a green co-precipitation approach, are included in the paper (Yin & Xu, 2020). The in situ azide alkyne cycloaddition process and the coupling reaction were used to examine the catalytic activity, and the reaction's temperature, solvent, and time were tuned. A synthesis of IONP and its application in cancer treatments studied in Arsalani et al. (2018); Popescu et al. (2020). The synthesized NPs used rosemary extract and cancer therapies by (Mahanty et al., 2019). In (2019), Cittrarasu, V. and others, Synthesis of Plant Extract Metal Nanoparticles and Application of MB Degradation (Cittrarasu et al., 2019). Nadeem et al. (2018) describe the green synthesis of metal nanoparticles from plant extract and their application in photocatalytic activity. A research team has invested in these waste materials, including rusty iron and aloe vera extract, which constitute a significant proportion globally. To remove the methylene blue dye in new research that has not yet been covered by any research group. The innovation of making use, without cost to manufacture value and valuable NP materials, of all the materials employed (which are first used as the authors' expertise). Furthermore, neither raw ingredients nor the final product are employed in this research. Without a supplement, all components used are natural. They were recycled into a very effective chemical to eliminate poisons and colors (MB dye). The research was carried out to mix iron scrap rust with aloe vera extract at (300 and 600) ^{o}C over 2 hours. IONPs were generated in this section. Treatment of environmental contaminants from MB dye under average light radiation using IONPs. (Fe_3O_4 and $Fe_{942}O$) were characterized via X-ray diffraction (XRD) and filed emission scanning electron scanning microscopy (FESEM). Further, the FTIR spectrum is used to determine the vibrations of mode and group functions. For the first time, researchers aim to synthesize IONPs with other plant extracts, but in this work, they utilize aloe vera gel extracts with rust iron. Which is the first time it is used as the author's acknowledgement. The photocatalytic activity of the produced nanoparticles was also tested for MB dye degradation.

2. MATERIALS AND METHODS

2.1. Experimental work

Our hypothesis is that several factors work together to determine the NPs synthesis, including plant source, extract, temperature, and time of reaction. The plant listed below is represented by Aloe vera Gel. This plant is rich in phenolic substances, especially quercetin, cardiac glycosides, phenolic acids, sulfur, compounds (allicin), alkaloids, flavonoids, terpenes, steroids, vitamins, and minerals. It is very rich in quercetin and fructose, which can reduce ions to NPs because of the presence of vitamin C in these plant extracts. As a first step, the plants were purchased at a market in Baghdad, Iraq.

2.2. Preparation of the aloe vera extract

Fresh aloe vera gel has been used in this study. 10 g of plants have been rinsed using filtered water to get rid of any dirt or dust, before being chopped up and blended into a fine powder. The plants were cooked in 100 mL of "distilled water" at 70 ^{o}C for 60 minutes. After that, we ran it through Whatman No. 4 filter paper (pore size 20 m) to remove any remaining debris. We then centrifuged the solution at "2000 rpm" for "10 minutes" to remove any remaining debris. Soon after being filtered, the plant extracts were employed in the green synthesis of NPs. Instructions for transforming raw plant material into an extract are provided in figure 1.

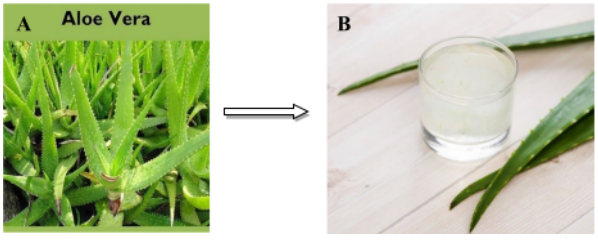

Figure 1. Shows the plant (*Aloe vera*) istransferred to the extract, A) aloe vera plant, and B) aloe vera extract.

2.3. Preparation of the rust iron extract

We take 148 g of iron rust to production IONPs. The iron scrap was cleaned with distilled water to remove the contaminants associated with it. The rust iron piece was then placed in a glass container with 500 ml of distilled water and exposed to the sun for five days. The red-colored, 250 ml sized rust iron extract was then collected and kept in sealed tubes for the manufacture of IO. Figure 2 (a–c) shows rust iron extract is created by combining distilled water with rust iron species.

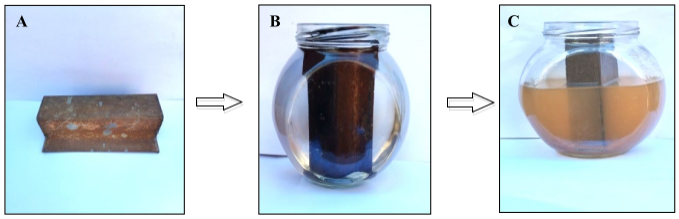

Figure 2. Transfer phases for five days of rust iron in sunlight extract: (a) rust iron species, (b) distillation ironspecies, and (c) rust iron extractor.

2.4. Preparation of (Fe_3O_4 and Fe_90_2O from the aloe vera extract and rust iron extract

This is created of IONPs by mixing 100 ml of aloe vera with 250 mL from a rusty iron extractor. The solution was then heated to 70°C on the hotplate stirrer for 60 minutes. It notices that, during synthesis, the color of the exhaust reaction quickly changed from transparent off-white to black and alludes to the formation of IONPs. The outcome was resolved at room temperature. To create the IONPs solution, 30 ml of IONPs were placed on a ceramic vine and heated to 200°C for 2 hours. Finally, sealed serum tubes were used to retain NP-solves of IO for further diagnosis, as shown in figure 3.

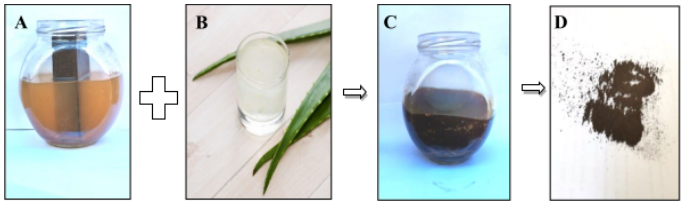

Figure 3. Figure 3: The transfer phase for five days is A) rust ironspecies, A) aloe vera extract, and C) IONPs powder.

2.5. IONP (Fe_3O_4 and Fe_90_2O characterization was generated using an extract (aloe vera

The specimen was determined using an XRD analysis of the results provided by the Joint Powder Diffraction Standards Committee (JCPDS) card. A step-by-step test model (XRD-6000, Shimadzu) application for 30 mA or 40 kV was collected between 10°-80° of the XRD measuring range. FESEM showed the diagnostic morphology and the size of the particle. FESEM (Tescan Mira3 FESEM, Czech Republic) in Iran-Mashhad was examined for the specimens. The absorption strength, the vibration mode, and function groups were investigated by FTIR spectra (Spectrum GX FT-IR, Perkin-Elmer).

2.6. Mechanism Interaction of Synthesis and Characterization of IONPs from Aloe Vera Extract by Hydrothermal Method as Determinants of Biologic Activity

FeO NPs have unique features due to their tiny size and correspondingly large specific surface area, such as their suitability as catalysts for chemical processes. Given that surface atoms or molecules dominate in defining bulk characteristics and that the proportion of surface to total atoms or molecules rises exponentially with decreasing particle size, the significance of surface area becomes clear. If NPs are ingested into live creatures, assuming they are solid rather than soluble particles, increased surface reactivity predicts that they will demonstrate more biologic activity per given mass than bigger particles (Amato, 1989). In addition, the analysis of the aloe vera extract revealed that it included various vitamins, enzymes, minerals, sugars, lignin, saponins, salicylic acids, and amino acids. Vitamins: It has antioxidant vitamins A (beta-carotene), C, and E. Additionally, it has vitamin B12, folic acid, and choline, which are crucial parts of henna extract. It also studies the breakdown of MB dye for environmental remediation using a hydrothermal approach. Due to the presence of polyphenols, antioxidants, and flavonoids, henna extract helps to transform iron rust into iron oxide nanoparticles (NPs); however, the precise process is still being studied (Abid & Kadhim, 2020). Equation (1) describes the chemical reaction of a mixture to produce FeO NPs. Figure 4 shows the mechanism-interaction of the synthesis and Characterization of IONPs from aloe vera extract by the hydrothermal method as determinants of biologic activity.Fe rest+ Plant extract (aloe veraFeO + HO FeO NPs (1)

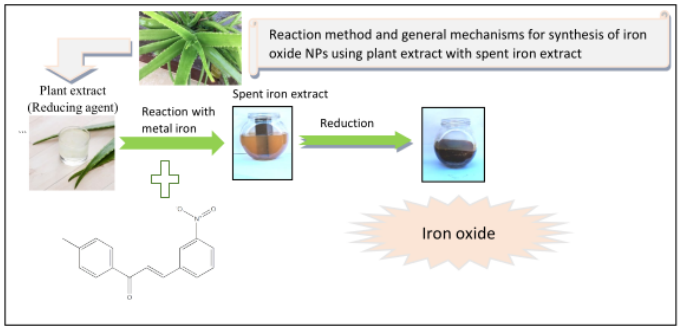

Figure 4. The interaction between the rust iron extract and the aloe vera extract.

2.7. The photocatalytic activity for degradation of MB dye using IONPs (Fe_3O_4 and Fe902O

In this study, IONPs are produced for the photo-catalytic action to remove MB coloring, resulting in a mixture of aloe vera extract and rust iron by the hydrothermal method at (300 and 600) °C. IONPs (Fe_3O_4 and $Fe_{902}O$) were used to remove MB dye under average light irradiation, and the process was done by mixing a specific amount of MB (0.001 g) with 100 ml of distilled water. After that, 0.003 g of IONPs powder was

scattered, and the solution was stirred by a hotplate stirrer for 10 minutes without light to preserve the IONPs solution's evenness. After 15 minutes, the mixture was put under direct, normal room light. Lastly, about 4 ml of solution was centrifuged at 10,000 rpm for 15 minutes. The specimen's absorbance was measured via the UV-Vis spectrum (Shimadzu, UV-1800), with the absorption maximum at λ = 664 nm. The following formula was used to determine the removal efficiency percentage of MB dye:

The efficiency of the formula (2) as used to remove MB dye is as follows:

$$The\ \ degradation\ efficiency\ (\%) = [C_{ini} - \frac{C_{fin}}{C_{ini}}] \times 100\ \% \quad (2)$$

Equation (3) was used to get the kinetic constant rate (Kph) of the degradation of the MB dye:

$$Ln\ [\frac{Cini}{Cfin}] = Kph \times t\ (3)$$

Equation (4) was used to determine the percentage of MB dye degradation that involves IONPs:

$$Percentage\ \ of\ \ degradation\ \ (\%) = [1 - \frac{Cini}{Cfin}] \times 100\% \ (4)$$

Where t is the exposure duration (in minutes), Kph is the kinetic rate constant (in minutes^{-1}), and C_{ini} and C_{fin} are the beginning and final concentrations of the MB dye, respectively.

3. RESULTS AND DISCUSSION

3.1. Synthesis and characterization of IONPs from the mixing of aloe vera with rust iron

It controlled the IONP creation rate, its fill, and its stability by adjusting the parameters of the aloe vera extract. Within an aloe vera extract, phytochemicals have the capacity to produce fewer iron ions in the short term. IONPs prepared from aloe vera minerals also play a crucial role in reducing and stabilizing these causes. Aloe vera extract comprises a range of anthraquinones, glucosidane, parabaloin, and an ingredient. It includes resin, organic and poly acids, aloe-emodins, and a few minerals. A gel in the aloe plant has been found in the leaves, and it has been demonstrated that this gel comprises 0.542% solids, 42% carbohydrates, 1.95% nitrogen, and 0.113% fatty compounds responsible for the production of IONPs.

3.2. Color Change

Through the visible color change, it can get first-hand information regarding the formation of IONPs. As the IONPs are created, the color of the solution changes from brown-red to black, which refers to the presence of IONPs. The various colors were due to the change in surface plasmon resonance of IONPs during their formation. The presence of the sources is due to the novelty of the work.

3.3. Weight Change

During the experiment, it was observed a loss in the weight of the rust iron, and this was done by measuring the weight of the piece of rust iron before use, and it was 148 g, and after its use, it became 147.01 g, and this is an indication of the disposal of rust iron and the formation of iron extract and their use in the preparation of IONPs. The presence of the sources is due to the novelty of the work.

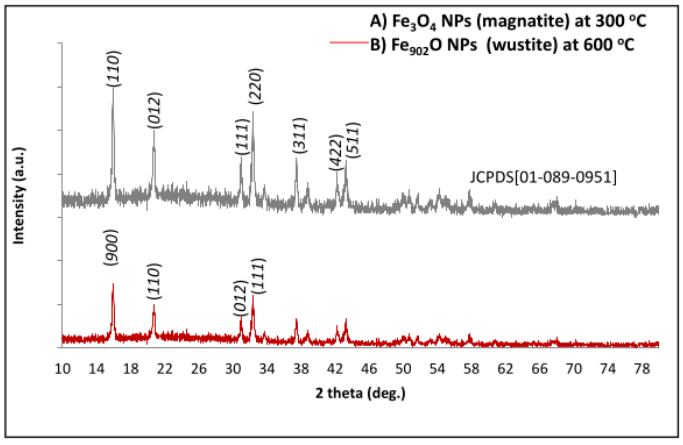

Figure 5. XRD analysis shows that the crystalline A) Fe_3O_4 (magnetites,space group of Fd-3m, JCPDS No. 01-089-0951) phase created by mixing the rustiron extract with aloe vera extract was produced at 300 °C, and (B) $Fe_{902}O$phase (wustite, space group of FM-3 m, JCPDS No. 01-079-1971) was produced at 600 °C.

3.4. XRD analysis of (Fe3O4 and Fe902O) produced from mixing the rust iron extract with aloe vera

XRD analysis is an excellent instrument utilized to determine samples in this research regarding material, structure, and orientation. IONPs were prepared by mixing the aloe vera with iron rust extract by the hydrothermal method at (300 and 600) °C, as shown in figures 5 (A–B). The high peaks of the crystalline Fe_3O_4 phase at (110) and (311) are indicated by (110), (012), (111), (220), (311), (422), and (511) of the miller (structure) indexes, as indicated by figure 5 (A) (Ramegowda & Senthil-Kumar, 2015; Sim et al., 2020). While the high peaks of the crystalline phase $Fe_{902}O$ are (006), (110), (012), and (111), miller indices with the face center cubic, as illustrated in figure 5 (B) (Maham et al., 2017; Popescu et al., 2020), the peaks of the crystalline phase $Fe_{902}O$ are (006) and (111). Table (1) provides the results in phases and crystalline IONPs (Fe_3O_4 and $Fe_{902}O$). The crystallite size D (nm) has been established by the following Scherrer formula 5 (Farshchi et al., 2018; Pawar et al., 2017):

$$D\ (nm) = \frac{k.\lambda}{\beta cos\theta}$$

When k is called a form factor, α is an angle of diffraction, and β is the total width of half (FWHM) (Cittrarasu et al., 2019); λ is the width of wavelength (0.15418) nm (CuKα). The XRD analytical data shows the stages (magnetic, Fd-3m, JCPDS 01-089-0951), prepared from mixing the rust iron extract with aloe vera at 300 °C, in an eco-friendly format and with the best possible orientation, compared with the crystalline $Fe_{902}O$ (Wustite, Fm-3m space groups, JCPDS no. 01-079-1971) prepared from mixing the rust iron extract with the aloe vera at 600 °C.

Table 1
XRD analysis shows the crystallite size forIONPs created from mixing the rust iron extract with aloe vera extract.

Plant extract	Materials	Temperature (^{o} C)	(hkl)	FWHM	Crystallite size D (nm)
Aloe vera	Fe_3O_4 (magnatite)	300	(110)	0.43	19
			(220)	0.30	26
	$Fe_{902}O$ (wustite)	600	(006)	0.28	28
			(111)	0.13	61

3.5. FE-SEM Images of IONPs (Fe_3O_4 and $Fe_{902}O$) from mixing the aloe vera extract with the rust iron

FE-SEM images illustrate the particle size and morphology of the surface area of environmentally friendly IONPs produced by mixing the aloe vera extract at (300 and 600) ^{o}C. The average grain volume is 26.80 to 37.96 nm, and the shape of the Fe_3O_4 NPs (magnetites) is 300 °C (nanosphere), as illustrated in figure 6 (A-B). The particle size and morphology of the $Fe_{902}O$ phase (wustite) are averaged (31.63 to 130.3), as is the (nano-inverse cubic) structure (as illustrated in figure 6 (A1-B1).

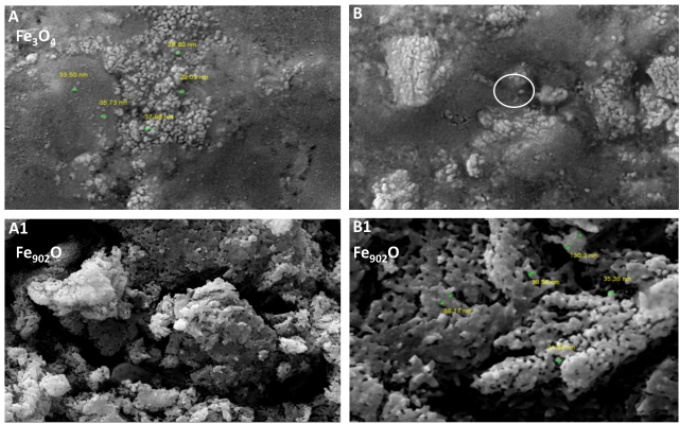

Figure 6. FE-SEM images illustrate the outcomes of IONPs generated from the aloe veraextract: A-B) Fe_3O_4 (magnetic) at 300°C, and A1-B1) $Fe_{902}O$NPs (wustite) at 600 ^{o}C.

FE-SEM images shows the particle size, and the morphology of environmentally compatible (Fe_3O_4) NPs (magnetites) made from mixing the rust iron extract with the aloe vera extract at 300 ^{o}C is better than those prepared for ($Fe_{902}O$) NPs (wustites) at 600 ^{o}C.K

3.6. FT-IR spectra of (Fe_3O_4 and Fe902O) produced from mixing rust iron with aloe vera

The FT-IR spectrum reveals the vibration and function groups of eco-friendly IONPs generated by the hydrothermal method from the rust iron extract with aloe vera at (300 and 600) ^{o}C. The absorption strength of the Fe_3O_4 NPs (magnetite, fingerprint area) is (660) cm^{-1} at 300 ^{o}C, as illustrated in figure 7 (A). In comparison, the absorption band is (650) cm^{-1} at 600 °C (wustite, fingerprint area), equivalent to Fe-O in $Fe_{902}O$ NPs, as shown in figure 7 (B).

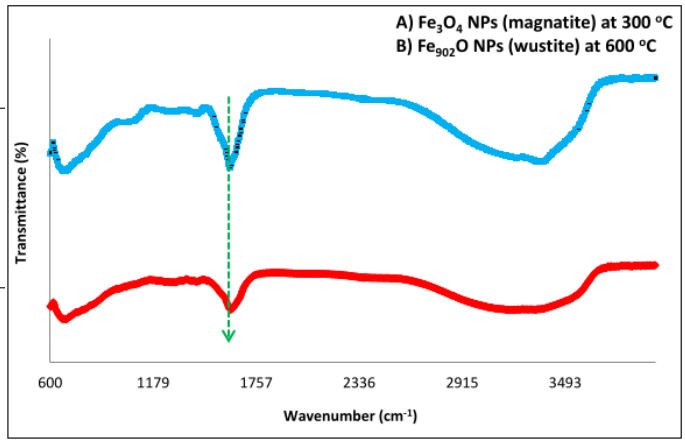

Figure 7. The FT-IR spectrum shows of the IONP preparation from mixing therust iron extract with aloe vera, A) Fe_3O_4 NPs (magnetite) at 300 ^{o}C, and B) $Fe_{902}O$ NP (Wustite) at 600 ^{o}C.

Table 2
The FTIR spectrum shows the values of IONPs from thealoe vera extract with the rust iron.

Plant extract	phases	Temperature ^{o} C	Absorption (cm^{-1})	Functional groups
Aloe vera	Fe_3O_4 (magnetite)	300	660	Fe-O
			1601	C=O, carbonyl
			3383	OH, hydroxide
	$Fe_{902}O$ (wustite)	600	650	Fe-O
			1566	C=C, isolated
			3289	OH, hydroxide

The FT-IR spectra show the absorption band of eco-conservative (Fe_3O_4) NPs (magnetites) produced by the aloe vera extract with the rust iron is increased by the hydrothermal method at 300 ^{o}C, then $Fe_{902}O$ at 600 ^{o}C.

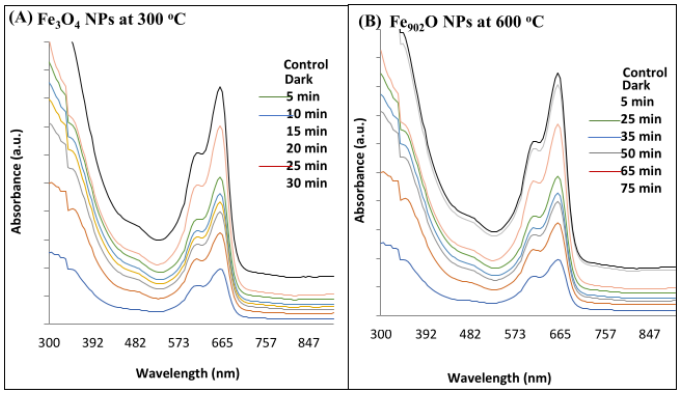

Figure 8. A) UV-Vis spectrum for MB dye removal down room light irradiation using Fe_3O_4 NPs (magnetite) at 300 ^{o}C,and B) $Fe_{902}O$ NPs (wustite) at 600 ^{o}C.

3.7. The photocatalytic activity for removal of MB dye using IONPs (Fe_3O_4 and Fe902O)

The application of IONPs prepared from mixing the aloe vera extract with rust iron extract for the MB dye removal. Figure

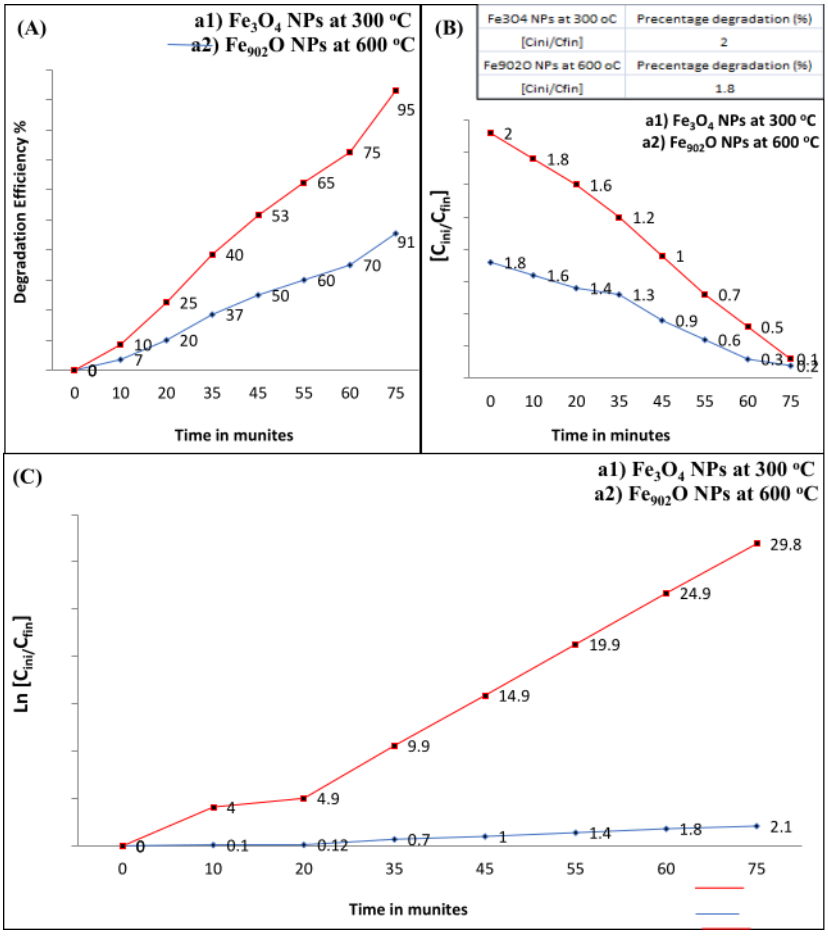

Figure 9. The efficiency of degradation (%) of MB dye is shownusing IONPs prepared by mixing the rust iron extract with aloe vera:(a1) Fe_3O_4 NPs at 300 °C and (a2) $Fe_{902}O$NPs at 600 °C, for the room condition. B) a pseudo kinetic curve forthe reaction of the first reaction for adsorption of MB applied (a1) Fe_3O_4NP at 300 °C, and (a2) $Fe_{902}O$ NP at 600 °C.

8 (A–B) showed the removal of MB dye without and using the (Fe_3O_4 and $Fe_{902}O$) NPs. The determination of MB dye removal using the (Fe_3O_4 and $Fe_{902}O$) NPs when exposed to natural light at room temperature is clean in figures 8 (A–B). When offering the dye to natural light irradiation, it notices that there is no change in the color and concentration of the dye, and they are still within the average extent. However, when the dye is mixed with IONPs under average light irradiation, it is observed that the dye's concentration gradually decreases until it is completely removed at the end (Kim et al., 2018; Singh et al., 2019a; Ullrich et al., 2019; Vaidyanathan et al., 2007). The reaction mechanism to remove the MB dye first occurs when $Fe_{902}O$ NPs with dye are exposed to natural light at normal conditions. An electron pair will generate a gap after the electrons are blustery from pupil conduction, and then holes are formed in the valence beam. Secondly, the holes form and the electrons interact with water and oxygen in the solution to produce the hydroxyl group, which is characterized by being highly oxidative. Finally, the resulting hydroxyl group obliterates the dye by extracting electrons from the dye molecules via breaking great organic matter into small, less harmful organic matter; this result is similar to the previous study (Dauthal & Mukhopadhyay, 2015; Devi et al., 2016; Khodadadi, 2017; Lassoued et al., 2019; Litvin & Minaev, n.d.; Singh et al., 2019b; Soltan et al., 2017; Yuan, 2018). Figure 8 (A-B) shows the removal efficiency (%) for MB dye-down natural light at the normal condition of IONPs created using aloe vera extract at (300 and 600) °C. The degradation efficiency (%) is (95 %) for 40 min of Fe_3O_4 NPs (magnetite) at 300 °C, but the degradation efficiency (%) was (91 %) for 75 min of $Fe_{902}O$ NPs at 600 °C, as shown in figure (A) (Zhang et al., 2011). The percentage of degradation MB dye that is degrading Fe_3O_4 NPs synthesized using aloe vera extract at 300 °C deposition on glass substrate by drop-casting method is higher than the percentage of degradation MB dye that is degrading $Fe_{902}O$ NPs using aloe vera extract at 600 °C, as explained in figure 9 (B) (Wilhelm et al., 2020). The constant rate Kph of MB dye of Fe_3O_4 NPs synthesized using the aloe vera extract at 300 °C deposition on glass substrate by the drop-casting method was determined to be 0.099 min^{-1}, but the constant rate Kph of MB dye of $Fe_{902}O$ NPs was 0.029 min^{-1}, as shown in figure 9 (C) (Ahmad et al., 2015; Brown, 1987; Ibrahim et al., 2013; Oelmüller, 2018; Reaad et al., 2023; Xu et al., 2012). IONPs are covered by the numerous phytochemicals found in

plant material. The ideal method is to use phytochemicals rather than other chemicals. These are simple to make and don't need to undergo high-temperature aloe vera material degradation in order to be used for this technique. Excellent dye degradation activity may be seen in them. These nanoparticles can be reused or recycled. When we add leaf extract from the aloe vera plant to the iron rust solution during the synthesis of the IONPs, the solution changes color and produces the IONPs. The IO surface was excited, which led to the creation of color. For the oxidation of the dye MB, highly active plant-assisted $Fe_{902}O$ NPs exhibit enhanced catalytic activity (Khalel et al., 2023).

4. CONCLUSION

This work has succeeded in producing IONPs (Fe_3O_4 and $Fe_{902}O$) by the hydrothermal method, utilizing modern methods of mixing plant extracts such as aloe vera and rust iron extract. XRD measurements explained the small size of the crystalline (19 nm) magnetite structure of (Fe_3O_4) NPs at 600 ^oC using aloe vera extract, while the tiny size of the crystalline ($Fe_{902}O$) NPs at 300 ^oC was at 28 nm. FE-SEM show the particle size of (Fe_3O_4) NPs at 600 °C for (26.80 to 37.96) nm, while the tiny crystalline size of the $Fe_{902}O$ NPs (wustite) at 300 °C was (31.63 to 130.3) nm. The FT-IR spectrum explains the strong absorption band of Fe_3O_4 NPs (magnetites) at 600 °C. The FT-IR spectra absorption band was (650) cm^{-1}, and were corresponding to Fe-O at 300 °C ($Fe_{902}O$ NP). In a relatively short time, IONPs for the breakdown of MB dye have been used in environmental treatment. The efficiency of degradation (percentage) for MB dye was 95% (40 minutes) for IONPs (Fe_3O_4) at 300 °C. In comparison, the efficiency of degradation (percent) for MB dye was 75 minutes (91%) with ($Fe_{902}O$) NPs at 600 °C. This work will provide us with wide-ranging new horizons to solve the problem of rust iron and how to remove it and produce new NPs when it comes to the environmental treatment of removing poisonous colors from water at accessible prices.

5. ACKNOWLEDGMENT

The author(s) would like to thank Mustansiriyah University (www.uomustansiriyah.edu.iq) Baghdad-Iraq for its support in the present work. We are thankful to head of the unviersity Proof. Hameed Fadhel Hasan.

CONFLICTS OF INTEREST

The authors declare that they have no known competing financial interests or personal relationships that could have influenced the work reported in this paper.

ORCID

Duha A. Kadhim 0009-0003-7012-5968
Muslim A. Abid 0000-0002-8158-3388
Wafaa Mahdi Salih 0000-0002-1069-5884

REFERENCES

Abid, M.A., Kadhim, D.A., 2020. Novel comparison of iron oxide nanoparticle preparation by mixing iron chloride with henna leaf extract with and without applied pulsed laser ablation for methylene blue degradation. Journal of Environmental Chemical Engineering. 8(5), 104138. https://doi.org/10.1016/j.jece.2020.104138

Ahmad, A., Mohd-Setapar, S.H., Chuong, C.S., Khatoon, A., Wani, W.A., Kumar, R., Rafatullah, M., 2015. Recent advances in new generation dye removal technologies: Novel search for approaches to reprocess wastewater. RSC Advances. 5(39), 30801. https://doi.org/10.1039/C4RA16959J

Aliasghari, S., Skeldon, P., Zhou, X., Gholinia, A., Zhang, X., Valizadeh, R., Withers, .., J, P., 2021. X-ray computed tomographic and focused ion beam/electron microscopic investigation of coating defects in niobium-coated copper superconducting radio-frequency cavities. Materials Chemistry and Physics. 273, 125062–125062. https://doi.org/10.1016/j.matchemphys.2021.125062

Amato, I., 1989. Making the right stuff. Science News. 136, 108–110. https://doi.org/10.2307/3973729

Arsalani, S., Guidelli, E.J., Araujo, J.F.D.F., Bruno, A.C., Baffa, O., 2018. Green Synthesis and Surface Modification of Iron Oxide Nanoparticles with Enhanced Magnetization Using Natural Rubber Latex. ACS Sustainable Chemistry & Engineering. 6, 13756–13765. https://doi.org/10.1021/acssuschemeng.8b01689

Bedin, K.C., Martins, A.C., Cazetta, A.L., Pezoti, O., Almeida, V.C., 2016. KOH-activated carbon prepared from sucrose spherical carbon: Adsorption equilibrium, kinetic and thermodynamic studies for methylene blue removal. Chemical Engineering Journal. 286, 476–484. https://doi.org/10.1016/j.cej.2015.10.099

Brown, D., 1987. Effects of colorants in the aquatic environment. Ecotoxicology and Environmental Safety. 13(2), 139–147. https://doi.org/10.1016/0147-6513(87)90001-7

Chamorro, E., Tenorio, M.J., Calvo, L., Torralvo, M.J., Sáez-Puche, R., Cabañas, A., 2020. One-step sustainable preparation of superparamagnetic iron oxide nanoparticles supported on mesoporous SiO2. The Journal of Supercritical Fluids. 159, 104775. https://doi.org/10.1016/j.supflu.2020.104775

Cittrarasu, V., Balasubramanian, B., Kaliannan, D., Park, S., Maluventhan, V., Kaul, T., Arumugam, M., 2019. Biological mediated Ag nanoparticles from Barleria longiflora for antimicrobial activity and photocatalytic degradation using methylene blue. Artificial Cells, Nanomedicine, and Biotechnology. 47(1), 2424–2430. https://doi.org/10.1080/21691401.2019.1626407

Cornell, R.M., Schwertmann, U., 2006. The Iron Oxides: Structure, Properties, Reactions, Occurrences and Uses, and others, (Eds.). John Wiley & Sons. 10.1002/3527602097

Dauthal, P., Mukhopadhyay, M., 2015. Agro-industrial waste-mediated synthesis and characterization of gold and silver nanoparticles and their catalytic activity for 4- nitroaniline hydrogenation. Korean Journal of Chemical Engineering. 32(5), 837–844. https://doi.org/10.1007/s11814-014-0277-y

Devi, T.B., Begum, S., Ahmaruzzaman, M., 2016. Photo-catalytic activity of plasmonic Ag@AgCl nanoparticles (synthesized via a green route) for the effective degradation of Victoria blue B from aqueous phase. Journal of Photochemistry and Photobiology B: Biology. 160, 260–270. https://doi.org/10.1016/j.jphotobiol.2016.03.033

Djilani, C., Zaghdoudi, R., Djazi, F., Bouchekima, B., Lallam, A., Modarressi, A., Rogalski, M., 2015. Adsorption of dyes on activated carbon prepared from apricot stones and commercial activated carbon. Journal of the Taiwan Institute of Chemical Engineers. 53, 112–121. https://doi.org/10.1016/j.jtice.2015.02.025

El-Baky, A., Senosy, R.M., Omara, E.M., Mohamed, W., Ibrahim, D.S.,

A, R., 2016. The Impact of the Implementation of Culture-based Antibiotic Policy on the Incidence of Nosocomial Infections in Neonates Hospitalized in Neonatal Intensive Care Unit in a general Egyptian hospital in upper Egypt. Journal of Pure and Applied Microbiology. 14(3), 1879–1892. https://doi.org/10.22207/JPAM.14.3.27

Fallah, M., Farzaneh, M., Yousefzadi, M., Ghorbanpour, M., Mirjalili, M.H., 2019. In vitro mass propagation and conservation of a rare medicinal plant, *Zhumeria majdae* Rech. f & Wendelbo (Lamiaceae). Biocatalysis and Agricultural Biotechnology. 17, 318–325. https://doi.org/10.1016/j.bcab.2018.12.010

Farshchi, H.K., Azizi, M., Jaafari, M.R., Nemati, S.H., Fotovat, A., 2018. Green synthesis of iron nanoparticles by Rosemary extract and cytotoxicity effect evaluation on cancer cell lines. Biocatalysis and Agricultural Biotechnology. 16, 54–62. https://doi.org/10.1016/j.bcab.2018.07.017

Ghayempour, S., Montazer, M., Rad, M.M., 2016. Encapsulation of Aloe Vera extract into natural Tragacanth Gum as a novel green wound healing product. International journal of biological macromolecules. 93, 344–349. https://doi.org/10.1016/j.ijbiomac.2016.08.076

Guo, J., Wang, R., Tjiu, W.W., Pan, J., Liu, T., 2012. Synthesis of Fe nanoparticles@ graphene composites for environmental applications. Journal of Hazardous Materials. 225, 63–73. https://doi.org/10.1016/j.jhazmat.2012.04.065

Herlekar, M., Barve, S., Kumar, R., 2014. Plant-mediated green synthesis of iron nanoparticles. Journal of Nanoparticles. 2014, 140614. https://doi.org/10.1155/2014/140614

Ibrahim, A.A.A.H., Al-Razak, A., Ibrahim, I.A., H, S., 2013. The Effect Of Tigris River Water Salinity On Corrosion Resistance Of Low Carbon Steel (St37). Journal of Engineering and Sustainable Development(5), 17–17.

Issa, B., Obaidat, I., Albiss, B., Haik, Y., 2013. Magnetic Nanoparticles: Surface Effects and Properties Related to Biomedicine Applications. International Journal of Molecular Sciences. 14(11), 21266–21305. https://doi.org/10.3390/ijms141121266

Kato, H., 2011. Tracking nanoparticles inside cells. Nature Nanotechnology. 6(3), 139–140. https://doi.org/10.1038/nnano.2011.25

Khalel, M.H., Hamza, A.F., Khaled, F., 2023. Water Harvesting in the Jimin Basin by Using Remote Sensing Techniques and Geographical Information Systems. Al-Mustansiriyah Journal of Science. 34(2), 25–31. https://doi.org/10.23851/mjs.v34i2.1301

Khatami, M., 2019. Super-paramagnetic iron oxide nanoparticles (SPIONs): greener synthesis using stevia plant and evaluation of its antioxidant propertiesm. Journal of Cleaner Production. 208, 1171–1177. https://doi.org/10.1016/j.jclepro.2018.10.182

Khodadadi, B., 2017. Hazelnut shell as a valuable bio-waste support for green synthesis of ag nps using *Origanum vulgare* leaf extract: Catalytic activity for reduction of methyl orange and congo red. Iranian Journal of Catalysis. 7(2), 111–119.

Kim, C., Lee, S.S., Lafferty, B.J., Giammar, D., Fortner, J., 2018. Engineered superparamagnetic nanomaterials for arsenic (V) and chromium (VI) sorption and separation: quantifying the role of organic surface coatings. Environmental Science: Nano. 5, 556–563. https://doi.org/10.1039/C7EN01006K

Lassoued, A., Lassoued, M.S., Dkhil, B., Gadri, A., Ammar, S., 2019. Synthesis, structural, optical and morphological characterization of hematite through the precipitation method: Effect of varying the nature of the base. Journal of Molecular Structure. 1141, 99–106. https://doi.org/10.1016/j.molstruc.2017.03.077

Litvin, V.A., Minaev, B.F., n.d.. The size-controllable, one-step synthesis and characterization of gold nanoparticles protected by synthetic humic substances. Materials Chemistry and Physics. 144(1-2), 168–178. https://doi.org/10.1016/j.matchemphys.2013.12.039

Maham, M., Nasrollahzadeh, M., Sajadi, S.M., Nekoei, M., 2017. Biosynthesis of Ag/reduced graphene oxide/Fe3O4 using *Lotus garcinii* leaf extract and its application as a recyclable nanocatalyst for the reduction of 4-nitrophenol and organic dyes. Journal of Colloid and Interface Science. 497, 33–42. https://doi.org/10.1016/j.jcis.2017.02.064

Mahanty, S., Bakshi, M., Ghosh, S., Chatterjee, S., Bhattacharyya, S., Das, P., Chaudhuri, P., 2019. Green Synthesis of Iron Oxide Nanoparticles Mediated by Filamentous Fungi Isolated from Sundarban Mangrove Ecosystem, India. BioNanoScience. 9, 638–651. https://doi.org/10.1007/s12668-019-00644-w

Maleki, A., Pajootan, E., Hayati, B., 2015. Ethyl acrylate grafted chitosan for heavy metal removal from wastewater: Equilibrium, kinetic and thermodynamic studies. Journal of the Taiwan Institute of Chemical Engineers. 51, 127–134. https://doi.org/10.1016/j.jtice.2015.01.004

Nadeem, M., Tungmunnithum, D., Hano, C., Abbasi, B.H., Hashmi, S.S., Ahmad, W., Zahir, A., 2018. The current trends in the green syntheses of titanium oxide nanoparticles and their applications. Green Chemistry Letters and Reviews. 11(4), 492–502. https://doi.org/10.1080/17518253.2018.1538430

Oelmüller, R., 2018. Sensing environmental and developmental signals via cellooligomers. Journal of Plant Physiology. 229, 1–6. https://doi.org/10.1016/j.jplph.2018.06.010

Pawar, R.C., Kang, S., Park, J.H., Kim, J.H., Ahn, S., Lee, C.S., 2017. Evaluation of a multi-dimensional hybrid photocatalyst for enrichment of H2 evolution and elimination of dye/non-dye pollutants. Catalysis Science & Technology. 7, 2579–2590. https://doi.org/10.1039/C7CY00466D

Popescu, R.C., Savu, D., Dorobantu, I., Vasile, B.S., Hosser, H., Boldeiu, A., Veldwijk, M.R., 2020. Efficient uptake and retention of iron oxide-based nanoparticles in HeLa cells leads to an effective intracellular delivery of doxorubicin. Scientific Reports. 10(1), 10530. https://doi.org/10.1038/s41598-020-67207-y

Rahmani, R., Gharanfoli, M., Gholamin, M., Darroudi, M., Chamani, J., Sadri, K., Hashemzadeh, A., 2020. Plant-mediated synthesis of superparamagnetic iron oxide nanoparticles (SPIONs) using aloe vera and flaxseed extracts and evaluation of their cellular toxicities. Ceramics International. 46(3), 3051–3058. https://doi.org/10.1016/j.ceramint.2019.10.005

Ramegowda, V., Senthil-Kumar, M., 2015. The interactive effects of simultaneous biotic and abiotic stresses on plants: Mechanistic understanding from drought and pathogen combination. Journal of Plant Physiology. 176, 47–54. https://doi.org/10.1016/j.jplph.2014.11.008

Reaad, S., Jasim, B.E., Aboud, N.A.A., Hussain, A.S., 2023. Activated Carbon Nanoparticles as Adsorbent to Remove the Cadmium Ion from Aqueous Solution: Thermodynamic Study. Al-Mustansiriyah Journal of Science. 34(2), 44–49. https://doi.org/10.23851/mjs.v34i2.1260

Ren, Y., Rahmani, H., Meletis, E.I., Zhang, Q., Cao, Y., 2021. A first-principles study of thiadiazole and dimercapto-thiadiazole adsorption on copper and silver surfaces. Materials Chemistry and Physics. 273, 125057–125057. https://doi.org/10.1016/j.matchemphys.2021.125057

Rominiyi, A.L., Shongwe, M.B., Ogunmuyiwa, E.N., Babalola, B.J., Lepele, P.F., Olubambi, P.A., 2020. Effect of nickel addition on densification, microstructure and wear behaviour of spark plasma sintered CP-titanium. Materials Chemistry and Physics. 240, 122130. https://doi.org/10.1016/j.matchemphys.2019.122130

Roy, S., Das, T.K., 2015. Plant mediated green synthesis of silver

nanoparticles-A. International Journal of Plant Biology & Research. 3, 1044–1055.
Samira, S.F., Carvalho., 2017. Dye degradation by green heterogeneous Fenton catalysts prepared in presence of *Camellia sinensis*. Journal of Environmental Management. 187, 82–88. https://doi.org/10.1016/j.jenvman.2016.11.032
Sharma, A., Verma, C., Mukhopadhyay, S., Gupta, A., Gupta, B., 2022. Development of sodium alginate/glycerol/tannic acid coated cotton as antimicrobial system. International Journal of Biological Macromolecules. 216, 303–311. https://doi.org/10.1016/j.ijbiomac.2022.06.168
Sim, Y.S., Yim, S.H., Choo, Y.S., 2020. Photosynthetic and Physiological Characteristics of the Evergreen *Ligustrum japonicum* and the Deciduous Cornus officinalis. Journal of Plant Biology. 64, 73–85. https://doi.org/10.1007/s12374-020-09284-0
Singh, A., Dwivedy, A.K., Singh, V.K., Upadhyay, N., Chaudhari, A.K., Das, S., Dubey, N.K., 2019a. Essential oils based formulations as safe preservatives for stored plant masticatories against fungal and mycotoxin contamination: A review. Biocatalysis and Agricultural Biotechnology. 17, 313–317. https://doi.org/10.1016/j.bcab.2018.12.003
Singh, A., Dwivedy, A.K., Singh, V.K., Upadhyay, N., Chaudhari, A.K., Das, S., Dubey, N.K., 2019b. Essential oils based formulations as safe preservatives for stored plant masticatories against fungal and mycotoxin contamination: A review. Biocatalysis and Agricultural Biotechnology. 17, 313–317. https://doi.org/10.1016/j.bcab.2018.12.003
Soltan, W.B., Lasssoued, M.S., Ammar, S., Toupance, T., 2017. Vanadium doped SnO2 nanoparticles for photocatalytic degradation of methylene blue. Journal of Materials Science: Materials in Electronics. 28, 15826–15834. https://doi.org/10.1007/s10854-017-7477-2
T, R., Reihaneh, N., 2021. The Interpretation of Graphical Features Applied to Mapping SWOT by the Architecture Students in the Design Studio. Journal of Design Studio. 3, 205–221. https://doi.org/10.46474/jds.1019310
Taghipour, F., 2004. Ultraviolet and ionizing radiation for microorganism inactivation. Water Research. 38(18), 3940–3948. https://doi.org/10.1016/j.watres.2004.06.016
Ullrich, A., Rahman, M.M., Longo, P., Horn, S., 2019. Synthesis and high-resolution structural and chemical analysis of iron-manganese-oxide core-shell nanocubes. Scientific Reports. 9(1), 19264–. https://doi.org/10.1038/s41598-019-55397-z
Vaidyanathan, G., Sendhilnathan, S., Arulmurugan, R., 2007. Structural and magnetic properties of Co1− xZnxFe2O4 nanoparticles by co-precipitation method. Journal of Magnetism and Magnetic Materials. 313, 293–299. https://doi.org/10.1016/j.jmmm.2007.01.010
Wilhelm, C., Goss, R., Garab, G., 2020. The fluid-mosaic membrane theory in the context of photosynthetic membranes: Is the thylakoid membrane more like a mixed crystal or like a fluid. Journal of Plant Physiology. 252, 153246. https://doi.org/10.1016/j.jplph.2020.153246
Xu, P., Zeng, G.M., Huang, D.L., Feng, C.L., Hu, S., Zhao, M.H., Lai, C., Wei, Z., Huang, C., Xie, G.X., Liu, Z.F., 2012. Use of iron oxide nanomaterials in wastewater treatment: A review. Science of The Total Environment. 424, 1–10. https://doi.org/10.1016/j.scitotenv.2012.02.023
Xue, T., Tang, K., Qi, W., Wei, Y., Ru, G., 2021. Tuning the electronic structure and optical properties of β-Te/g-SiC and β-Te/MoS2 van der Waals heterostructure. Materials Chemistry and Physics. 273, 125026. https://doi.org/10.1016/j.matchemphys.2021.125026
Yew, Y.P., Shameli, K., Miyake, M., Khairudin, N., Mohamad, S., Naiki, T., Lee, K.X., 2018. Green biosynthesis of superparamagnetic magnetite Fe3O4 nanoparticles and biomedical applications in targeted anticancer drug delivery system: a review. Arabian Journal of Chemistry. 13, 2287–2308. https://doi.org/10.1016/j.arabjc.2018.04.013
Yin, J., Xu, L., 2020. Batch preparation of electrospun polycaprolactone/chitosan/aloe vera blended nanofiber membranes for novel wound dressing. International journal of biological macromolecules. 160, 352–363. https://doi.org/10.1016/j.ijbiomac.2020.05.211
Yuan, J., 2018. Two Dimensional Materials for Renewable Energy Harvesting and Energy Efficient Devices,. . https://hdl.handle.net/1911/105667
Zhang, Y.C., Du, Z.N., Li, K.W., Zhang, M., Dionysiou, D.D., 2011. High-performance visible-light-driven SnS2/SnO2 nanocomposite photocatalyst prepared via in situ hydrothermal oxidation of SnS2 nanoparticles. ACS Applied Materials & Interfaces. 3, 1528–1537. https://doi.org/10.1021/am200102y
Zhao, B., He, M., Chen, B., Hu, B., 2018. Ligand-assisted magnetic solid phase extraction for fast speciation of silver nanoparticles and silver ions in environmental water. Talanta. 183, 268–275. https://doi.org/10.1016/j.talanta.2018.02.081